ACS Sustainable Chemistry & Engineering

Research Article

pubs.acs.org/journal/ascecg

Stabilization Mechanisms and Reaction Sequences for Sintering Simulated Copper-Laden Sludge with Alumina

Yuanyuan Tang and Kaimin Shih*

Department of Civil Engineering, The University of Hong Kong, Pokfulam Road, Hong Kong SAR, China

Supporting Information

ABSTRACT: To stabilize copper-laden sludge using alumina-based ceramic raw materials, this study quantifies the copper transformation behavior during the sintering process. Results indicate crystallochemical incorporation of hazardous copper through the formation of copper aluminate spinel ($CuAl_2O_4$) and cuprous aluminate ($CuAlO_2$). To quantify the copper transformation and reveal reaction sequences, CuO was mixed with γ-Al_2O_3 and α-Al_2O_3 precursors and fired at 1050−1150 °C for 15−180 min. The sintered products were examined using X-ray diffraction (XRD), and copper transformations into both aluminate phases were quantitatively determined through Rietveld refinement analysis of XRD data. When γ-Al_2O_3 was used, $CuAlO_2$ was predominately generated from $CuAl_2O_4$ decomposition. However, $CuAlO_2$ was largely generated by the interaction between CuO and α-Al_2O_3. This study also compared the sintering behavior of both precursor systems and observed the relatively slower decomposition of $CuAl_2O_4$ in the γ-Al_2O_3 system. The reoxidation of $CuAlO_2$ into $CuAl_2O_4$ with an extended sintering time was detected in the α-Al_2O_3 system. The sample leachability analysis reveals that both $CuAl_2O_4$ and $CuAlO_2$ structures were superior in copper stabilization compared to the oxide forms. Such results suggest reliable mechanisms of incorporating hazardous copper into a ceramic matrix and demonstrate the potential of using waste materials as part of ceramic raw materials to produce detoxified products.

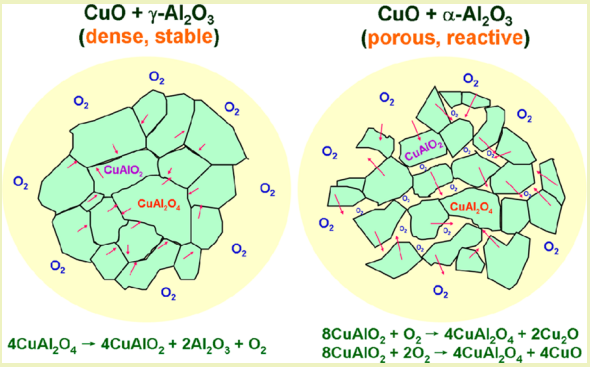

KEYWORDS: *Copper aluminate, Reaction sequences, Stabilization, Sintering, Leaching behavior, Waste-to-resource*

INTRODUCTION

Hazardous metals such as copper in wastewater can be rapidly removed by settling particulates, such as through the processes of precipitation, coagulation, reduction, ion exchange, and membrane processes,[1] to result in waste sludge containing hazardous metals. Hazardous metal-containing sludge needs to be disposed of in controlled landfills. However, the high cost of this strategy, combined with the limited number of landfills capable of accepting toxic metal waste, has made the development of effective and economical treatment strategies essential. The fabrication of a variety of ceramic products (bricks, tiles, and refractory aggregates) from metal-containing waste materials using a thermal process has been reported as a promising approach to the effective stabilization of hazardous metals.[2,3] In previous sintering studies,[4−7] preliminary investigations aiming to remove hazardous metals from the waste stream by blending them into marketable ceramic products were carried out. The simulated nickel- and copper-sludge materials were found to be able to react with the common components of ceramic raw materials, such as alumina, hematite, and kaolinite, to form spinel phases (AB_2O_4; A is a divalent metal and B is a trivalent metal) during the sintering process. In addition, the results suggested that the metal leachability of the sintered product phases could be substantially reduced due to the formation of such spinel phases after thermal treatment.[6,7]

In copper-laden sludge, copper carbonate, sulfate, and hydroxide are often the main copper-containing phases. The metals in sludge are generally transferred into their respective metal oxides after being heated at high temperatures. A copper-laden industrial sludge was collected, and CuO was found to be the main copper phase after calcining the sludge at 900 °C for 1 h (Figure S1, Supporting Information). Therefore, CuO was used in this study to observe its interaction with γ-Al_2O_3 and α-Al_2O_3 during the sintering process. The equilibrium phase diagram of the CuO−Al_2O_3 binary system[8] indicates that two aluminates ($CuAl_2O_4$ and $CuAlO_2$) can coexist in a mixture of CuO and alumina heated to temperatures above 1000 °C. However, because the dwelling time of the ceramic sintering process can vary from a few minutes to several hours,[9−12] the metal incorporation reactions are kinetically limited. The dominant mechanism for hosting copper in crystal structures under different thermal conditions should be unambiguously identified, if not also quantitatively evaluated. Metal hosting phases can be identified by comparing the X-ray diffraction

Received: March 22, 2013
Revised: June 3, 2013
Published: July 15, 2013

 © 2013 American Chemical Society

(XRD) profiles of samples to the standard diffraction patterns of potential crystal phases. Quantitative phase composition can be estimated using XRD data and the Rietveld refinement technique,[13−15] which consists of fitting the complete experimental diffraction pattern with a calculated profile.[16,17] Both qualitative and quantitative information on the key processes of incorporating hazardous metals into ceramic matrices can be provided to facilitate the reliable optimization of sintering processes.

Although the aforementioned equilibrium study has indicated potential for forming copper aluminates from a CuO + Al_2O_3 system, the reaction sequences involved in the incorporation of copper at different temperatures and alumina precursors (γ-Al_2O_3 and α-Al_2O_3) are still not clear. In this study, the effects of thermally incorporating CuO (simulated copper-laden sludge under a high temperature environment) into γ-Al_2O_3 and α-Al_2O_3 (corundum) ceramic precursors were investigated using a 3 h sintering scheme at temperatures between 650 and 1150 °C. The dominant reaction mechanisms at different sintering periods were quantitatively determined together with the influence of the sintering temperature. Furthermore, the stabilization effects of all of the copper-containing phases in the product were evaluated via a prolonged leaching experiment modified from the U.S. EPA's Toxicity Characterization Leaching Procedure (TCLP). The obtained leachability of each phase was further normalized using the sample surface area and copper content to reflect the intrinsic copper leachability and suggest a more reliable way to host the hazardous copper.

EXPERIMENTAL SECTION

In a high temperature environment, the copper content in sludge is mostly transformed into its oxide form as described in the Introduction. CuO powder with an average particle size (d_{50}) of 18.8 μm was purchased from Sigma Aldrich. The γ-Al_2O_3 was prepared using HiQ-7223 alumina powder (Alcoa Corp.) with an average particle size (d_{50}) of 53.1 μm. A qualitative phase identification of HiQ-7223 alumina was conducted using the powder XRD technique, and the result indicated a boehmite (AlOOH) phase composition. Boehmite was reported to convert to γ-Al_2O_3 upon thermal treatment at 650 °C for 3 h,[18] with the further calcination of as-formed γ-Al_2O_3 at 1500 °C for 6 h producing corundum as another copper stabilization precursor. The phase confirmation for these three raw materials was demonstrated by their XRD patterns, which are provided in Figure S2 of the Supporting Information. The samples used for the incorporation experiment were prepared by mixing each precursor with CuO for a total dry weight of 120 g at a molar ratio of Cu:Al = 1:2. The mixing process was carried out by ball milling the powder in a water slurry for 18 h to homogenize the particle sizes of different raw material mixtures into a size range at around 10 μm as shown in Figure S3 of the Supporting Information. The dry samples were then pressed into 20 mm pellets at 650 MPa and fired in a top-hat furnace (LHT 02/16 LB, LBR, Nabertherm, Inc.).

Phase transformation during sintering was monitored using the powder XRD technique. The step-scanned XRD pattern of each powder sample was recorded using a Bruker D8 Advance X-ray powder diffractometer equipped with Cu K$\alpha_{1,2}$ X-ray radiation (40 kV 40 mA) and a LynxEye detector. The 2θ scanning range was 10−90°, and the step size was 0.02° with a scan speed of 0.3 s step^{-1}. The qualitative phase identification was executed by matching powder XRD patterns with those retrieved from the International Centre for Diffraction Data's standard powder diffraction database (ICDD PDF-2 Release 2008). Four copper-containing crystalline phases were found in the products of this study, including CuO (PDF #80-1268), $CuAl_2O_4$ (PDF #33-0448), $CuAlO_2$ (PDF #75-1988) and Cu_2O (PD F#78-2076). They were all subjected to quantitative phase analysis together with the remaining corundum phase (PDF #10-0173) in the system using Topas 4.2, a program that employs the Rietveld refinement method. To assess the validity of the refinement procedure in quantifying the crystalline phases found in this study, solid mixtures containing authentic CuO, $CuAl_2O_4$, $CuAlO_2$, and α-Al_2O_3 in known weight fractions were tested with satisfactory results (Table S1, Supporting Information).

All of the copper-containing phases that had the potential of appearing in the sintered products of this study were tested using a prolonged leaching experiment to evaluate their copper leachability. The prolonged leaching experiment was modified from the U.S. EPA SW-846 Method 1311, Toxicity Characteristic Leaching Procedure (TCLP), with a pH 2.9 acetic acid solution (extraction fluid #2) as the leaching fluid. Each leaching vial was filled with 10 mL of TCLP extraction fluid and 0.5 g of powder. The leaching vials were then rotated end-over-end at 60 rpm for agitation periods of 0.75 to 22 d. At the end of each agitation period, the leachates were filtered with 0.2 μm syringe filters. The pH was measured via a pH meter (Thermo Scientific), and the concentrations of all metals were derived using ICP-AES (Perkin-Elmer Optima 3300 DV).

RESULTS AND DISCUSSION

$CuAl_2O_4$ Spinel Formation and Decomposition. The powder XRD patterns illustrated in Figures 1 and 2 indicate

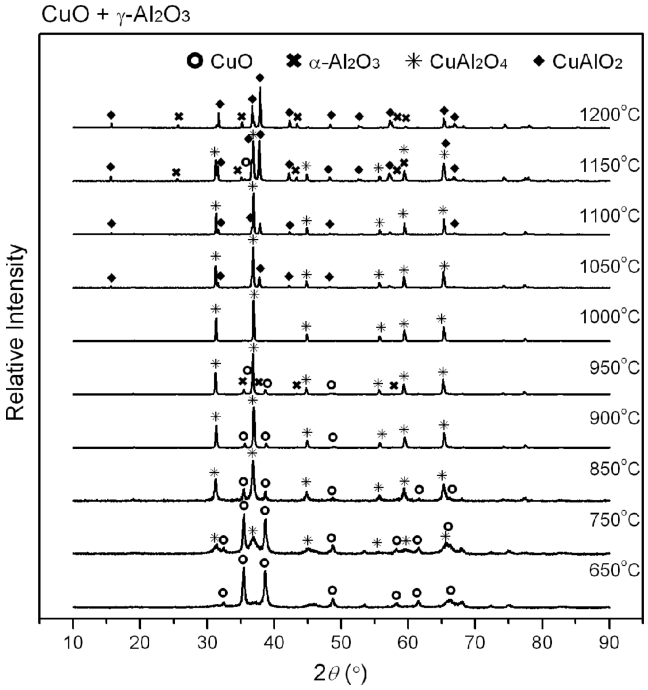

Figure 1. XRD patterns for the sintered CuO + γ-Al_2O_3 samples showing the thermal incorporation of copper within sintering temperatures ranging from 650 to 1200 °C for 3 h.

that copper can be successfully incorporated into a $CuAl_2O_4$ structure using γ-Al_2O_3 and α-Al_2O_3 precursors within a 3 h sintering scheme. With sintering temperatures ranging from 650 to 1200 °C, the XRD patterns revealed a distinguishable $CuAl_2O_4$ crystalline phase in the γ-Al_2O_3 precursor system after the 750 °C sintering (Figure 1). Sintering conducted at temperatures below 1000 °C revealed an increase in $CuAl_2O_4$ peak intensity with increasing temperature. However, when the sintering temperature was higher than 1000 °C, the peak intensity of the $CuAl_2O_4$ phase decreased with elevated temperature. When using α-Al_2O_3 as a precursor, the $CuAl_2O_4$ phase appeared at 900 °C and developed until the

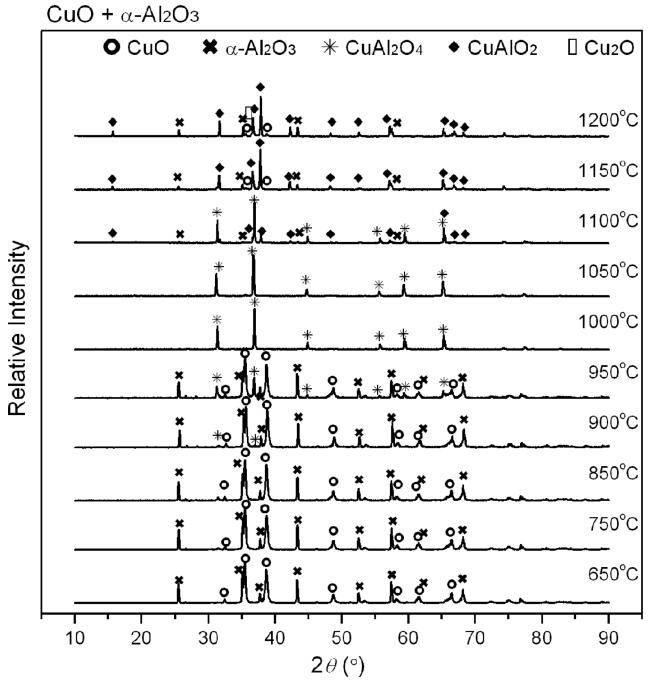

Figure 2. XRD patterns for the sintered CuO + α-Al_2O_3 (corundum) samples showing the thermal incorporation of copper within sintering temperatures ranging from 650 to 1200 °C for 3 h.

temperature reached 1050 °C. However, the diffraction peak of the $CuAl_2O_4$ phase nearly disappeared at the sintering temperature higher than 1150 °C (Figure 2). The chemical reactions for the formation of $CuAl_2O_4$ using γ-Al_2O_3 or α-Al_2O_3 as the precursor can be formulated as follows[6,8]

$$CuO + Al_2O_3 \rightarrow CuAl_2O_4 \quad (1)$$

With the reduction in $CuAl_2O_4$ at high temperatures, the growth of another new aluminate phase, $CuAlO_2$ (cuprous aluminate), was observed in the XRD patterns at high temperatures in the γ-Al_2O_3 and α-Al_2O_3 systems (Figures 1 and 2). The decomposition of $CuAl_2O_4$ spinel and the subsequent formation of the $CuAlO_2$ phase with an increase in sintering temperature was also found by previous studies[8,19] According to the diffraction pattern database, the predominant peaks of $CuAl_2O_4$ (PDF #33-0448) and $CuAlO_2$ (PDF #75-1988) are mainly located in the 2θ range from 30.0 to 46.0°. Therefore, Figure 3 provides a detailed XRD pattern comparison in the 2θ range to monitor the phase transformation process of $CuAl_2O_4$ and $CuAlO_2$ at higher temperatures. As a decrease in $CuAl_2O_4$ at high temperatures was accompanied by a corresponding increase in $CuAlO_2$ within the system, the formation of $CuAlO_2$ is likely to have occurred immediately after the decomposition of $CuAl_2O_4$ or must have gone through structural transformation by discharging the excessive aluminum and oxygen from the crystal structure. Together with the interaction between unreacted CuO and Al_2O_3,[8,19] the $CuAlO_2$ formation mechanisms can be organized as follows

$$4CuAl_2O_4 \rightarrow 4CuAlO_2 + 2Al_2O_3 + O_2 \quad (2)$$

$$4CuO \rightarrow 2Cu_2O + O_2 \quad (3)$$

$$Cu_2O + Al_2O_3 \rightarrow 2CuAlO_2 \quad (4)$$

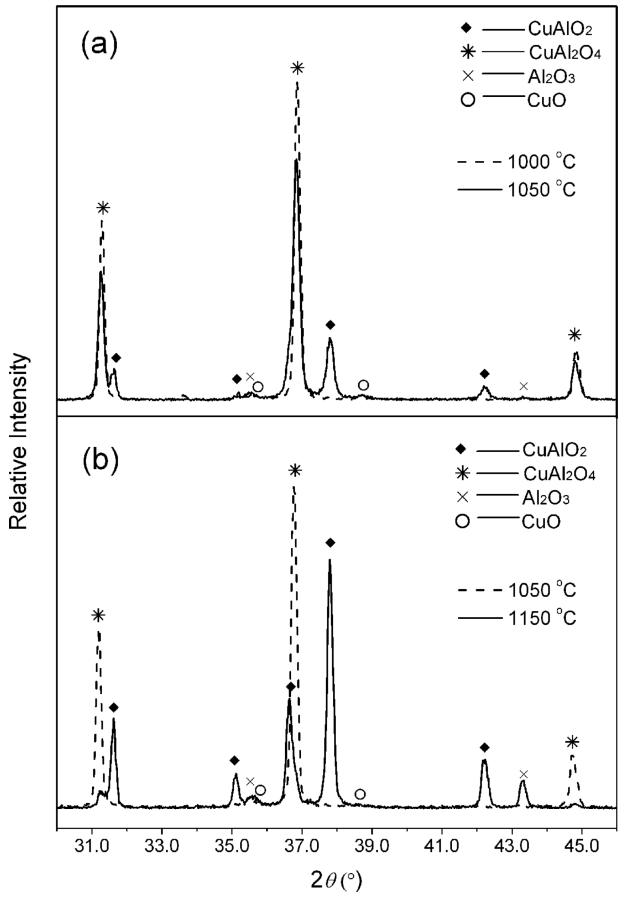

Figure 3. XRD patterns showing the thermal decomposition of $CuAl_2O_4$ and the formation of $CuAlO_2$ in the (a) CuO + γ-Al_2O_3 and (b) CuO + α-Al_2O_3 (corundum) systems.

Reaction Sequences within γ-Al_2O_3 and α-Al_2O_3 Systems. The appearance of the $CuAlO_2$ phase was either the result of the decomposition of $CuAl_2O_4$ or the reaction between Cu_2O and Al_2O_3. However, the predominant reaction mechanism and sequence in the early sintering stage have rarely been investigated. Therefore, temperatures of 1050, 1100, 1150, and 1200 °C were selected with sintering times of 15, 30, 60, 90, 120, and 180 min, respectively, to reveal the details of the copper transformation processes in the early stages of the γ-Al_2O_3 and α-Al_2O_3 precursor systems.

Rietveld refinement was applied to the XRD patterns of the sintered samples to quantitatively express copper transformation efficiency. The weight percentages of the crystalline phases in the samples from the CuO + γ-Al_2O_3 and CuO + α-Al_2O_3 systems are illustrated in Figure 4. After sintering at 1050 °C for 15 min, the $CuAl_2O_4$ spinel phase dominated as much as 90 wt % in the product of the γ-Al_2O_3 system (Figure 4a). However, the $CuAl_2O_4$ phase then decreased with the increase of $CuAlO_2$ at longer sintering times, which is consistent with the decomposition of $CuAl_2O_4$ into $CuAlO_2$ as described in eq 2. When samples were sintered at 1100, 1150, and 1200 °C, $CuAl_2O_4$ and $CuAlO_2$ coexisted in the samples, even within the first 15 min. At all of the sintering temperatures, the weight percentage of $CuAl_2O_4$ decreased consistently with the increase in $CuAlO_2$ at prolonged sintering times. This result reflects an important $CuAlO_2$ formation mechanism resulting from the decomposition of $CuAl_2O_4$ as described in eq 2. At 1200 °C,

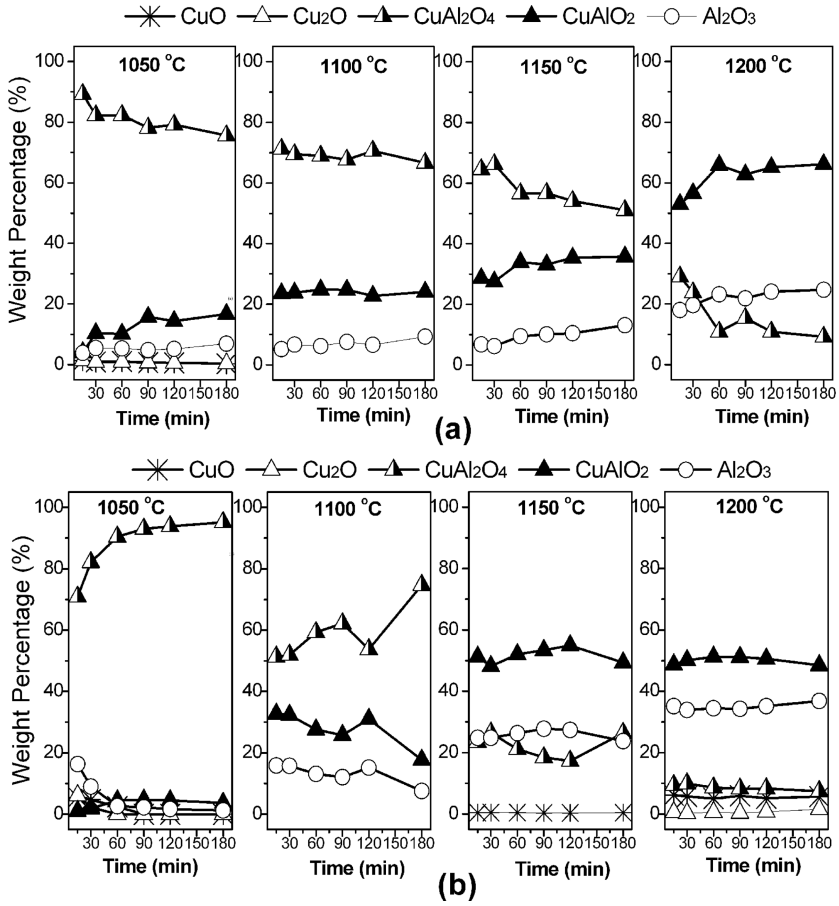

Figure 4. Sintering from 1050 to 1200 °C, the weight fractions of Cu- and Al-containing crystalline phases in the systems of CuO + (a) γ-Al_2O_3 and (b) α-Al_2O_3 precursors varied at different sintering times.

$CuAlO_2$ even became the predominant copper-hosting phase and took up to around 60 wt % in the product.

Figure 4b displays the variations in crystalline phases produced by using corundum as the precursor. Upon heating at 1050 °C, the weight percentage of the $CuAl_2O_4$ phase increased from 70% in the first 15 min to around 90% after 60 min. Simultaneously, the appearance of $CuAlO_2$ in the system was likely due to the interaction between Cu_2O and Al_2O_3, as reported by thermogravimetry (TG) and differential thermal analysis (DTA) studies at temperatures above 1000 °C.[19] Within the first 15 min of the 1100 °C sintering process, about 50 wt % of the $CuAl_2O_4$ phase was found in the product, together with 30 wt % of the $CuAlO_2$ phase. An increase in $CuAl_2O_4$ spinel and a corresponding decrease in the $CuAlO_2$ phase were observed with the extended sintering time. The 1100 °C process was reported to be near the boundary between the CuO and Cu_2O phases,[8,20] such that the potential reduction of Cu to Cu(I) led to a $CuAlO_2$ product after reacting with the available Al_2O_3. Moreover, Susnitzky[20] found that the $CuAlO_2$ structure might also decompose through the following reactions

$$8CuAlO_2 + O_2 \rightarrow 4CuAl_2O_4 + 2Cu_2O \quad (5)$$

or

$$8CuAlO_2 + 2O_2 \rightarrow 4CuAl_2O_4 + 4CuO \quad (6)$$

In this study, the CuO and Cu_2O generated from the above reactions should have already reacted with the remaining Al_2O_3 in the system to form copper aluminate again. The reoxidation of Cu(I) into Cu(II) in oxide form has also been reported by Tsuchida[19] during the experimental transformation of CuO to Cu_2O under high temperatures. Moreover, because $O_{2(g)}$ is required to participate in eqs 5 and 6, the $O_{2(g)}$ supply channels for initiating the formation of $CuAl_2O_4$ are crucial. Our previous study found a highly porous microstructure of products sintered from the CuO + α-Al_2O_3 system, compared to the commonly found dense form derived from the CuO + γ-Al_2O_3 system.[7] Therefore, samples from the CuO + α-Al_2O_3 system had a much higher chance of obtaining O_2 to facilitate the reactions in eqs 5 and 6, which led to an increase in $CuAl_2O_4$ during prolonged sintering. At higher temperatures, such as 1150 and 1200 °C, the Cu(II) was highly transformed to Cu(I), and the predominant Cu-hosting phase was $CuAlO_2$.

Figure S4 of the Supporting Information compares the effects of sintering temperature at the same dwelling time and reflects the decrease in the $CuAl_2O_4$ spinel phase with the corresponding increase in $CuAlO_2$ under elevated sintering temperatures. Below 1050 °C, the peak intensity of the $CuAl_2O_4$ phase increased with an increase in sintering temperature in both systems (Figures 1 and 2). With γ-Al_2O_3 as the precursor, the $CuAl_2O_4$ spinel phase decreased from ~90% to ~30% from 1050 to 1200 °C, respectively, even within a short 15 min sintering. While in the α-Al_2O_3 system, a more significant decrease in the $CuAl_2O_4$ spinel phase was observed from ~90% to ~10%. Consequently, the phase compositions of the $CuAlO_2$ phase increase to ~60% in both systems. Although the decomposition of the $CuAl_2O_4$ spinel phase was observed in both precursor (γ-Al_2O_3 and α-Al_2O_3)

systems, the decomposition of the $CuAl_2O_4$ spinel phase within 1050−1150 °C occurred much more slowly when γ-Al_2O_3 was used as the precursor. However, this situation reverses at higher temperatures (1150−1200 °C), such that the decomposition of $CuAl_2O_4$ was slower with the α-Al_2O_3 precursor. Overall, when using γ-Al_2O_3 as a precursor, the decomposition of $CuAl_2O_4$ at higher temperatures (>1150 °C) was more significant. For the CuO + α-Al_2O_3 system, the decomposition of $CuAl_2O_4$ is more significantly influenced by the sintering temperature at the relatively lower temperature range.

Copper Incorporation Efficiency with γ-Al_2O_3 and α-Al_2O_3 Precursors. As $CuAl_2O_4$ and $CuAlO_2$ were the predominant copper-hosting phases, the copper incorporation efficiencies into these two phases were quantitatively analyzed in the γ-Al_2O_3 and α-Al_2O_3 precursor systems. In this study, the transformation ratio (TR) used to indicate the extent of the copper incorporation efficiencies generated by the incorporation reactions reported in this study was defined to more clearly compare the effectiveness of metal stabilization. The TR values of copper incorporation into $CuAl_2O_4$ and $CuAlO_2$ were calculated as TR_s and TR_d, respectively

$$TR_s(\%) = \frac{\frac{\text{wt \% of } CuAl_2O_4}{\text{MW of } CuAl_2O_4}}{\frac{\text{wt \% of } CuAl_2O_4}{\text{MW of } CuAl_2O_4} + \frac{\text{wt \% of CuO}}{\text{MW of CuO}} + 2 \times \frac{\text{wt \% of } Cu_2O}{\text{MW of } Cu_2O} + \frac{\text{wt \% of } CuAlO_2}{\text{MW of } CuAlO_2}} \quad (7)$$

or

$$TR_d(\%) = \frac{\frac{\text{wt \% of } CuAlO_2}{\text{MW of } CuAlO_2}}{\frac{\text{wt \% of } CuAl_2O_4}{\text{MW of } CuAl_2O_4} + \frac{\text{wt \% of CuO}}{\text{MW of CuO}} + 2 \times \frac{\text{wt \% of } Cu_2O}{\text{MW of } Cu_2O} + \frac{\text{wt \% of } CuAlO_2}{\text{MW of } CuAlO_2}} \quad (8)$$

where MW = molecular weight, and a TR value of 100% represents the complete transformation of copper into a $CuAl_2O_4$ or $CuAlO_2$ phase.

Figure 5a shows that the TR_s values for the CuO + γ-Al_2O_3 system decreased with an increase in temperature, and the equilibrium was usually reached within a short sintering time except at the highest temperature of 1200 °C. In contrast, the TR_s values for the CuO + α-Al_2O_3 system decreased more rapidly with the same increase in temperature, but the sintering time generally enhanced the copper incorporation into $CuAl_2O_4$. A similar time-response behavior with a reversed development trend was found for the TR_d values shown in Figure 5b. As temperature increased, the gradual increase in TR_d in the CuO + γ-Al_2O_3 system generally stabilized within a short sintering period. The effects of sintering temperature were also more prominent in the CuO + α-Al_2O_3 system. The decrease in TR_s values, together with the complementary increase in TR_d over an extended sintering time in the CuO + γ-Al_2O_3 system confirms the $CuAl_2O_4$ decomposition to $CuAlO_2$ mechanism, which was particularly more intensive at the highest temperature of 1200 °C. In the α-Al_2O_3 system, the reoxidation of $CuAlO_2$ into $CuAl_2O_4$ during the extended sintering time can be further demonstrated by the increase in TR_s and decrease in TR_d values.

In the initial sintering stage, the use of γ-Al_2O_3 usually achieved a higher $CuAl_2O_4$ transformation (TR_s) compared to the use of α-Al_2O_3. With distinctly different crystal structures

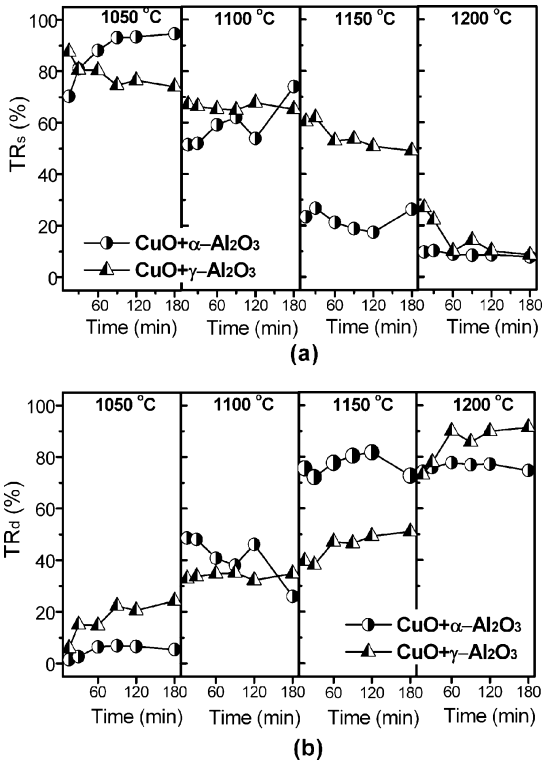

Figure 5. Transformation ratios (TR) of copper into the (a) $CuAl_2O_4$ (TR_s) and (b) $CuAlO_2$ (TR_d) phases under different sintering conditions. The sintering temperature ranged from 1050 to 1200 °C, and the sintering time ranged from 15 to 180 min.

between γ-Al_2O_3 and α-Al_2O_3,[21] the formation of $CuAl_2O_4$ spinel requires substantial oxygen repacking from an α-Al_2O_3 precursor structure, whereas the γ-Al_2O_3 precursor already has a spinel structure. In addition, the driving forces of mass transfer during the sintering process are related to the differences in chemical potentials (free enthalpy or molar Gibbs energy) between reactants.[22] The value of ΔH_f° (standard enthalpy of formation) for γ-Al_2O_3 is 18.8 kJ mol^{-1} higher than that of corundum,[23] and thus the reaction between CuO and γ-Al_2O_3 is more energetically favorable compared to that between CuO and α-Al_2O_3. In addition, the results in Figure 5 also reflect a more sensitive phase transformation behavior response to sintering temperature and time in the α-Al_2O_3 precursor system. As reported in our previous studies,[4,5,7] the $CuAl_2O_4$/$CuAlO_2$ pellets sintered using the α-Al_2O_3 precursor clearly had a very porous microstructure compared to that of the densely packed grains sintered using the γ-Al_2O_3 precursor. The dense microstructure of the products in the γ-Al_2O_3 precursor system indicates a greater diffusion barrier to the phase transformation process, induced by temperature change and prolonged sintering time. Therefore, the sensitivity of the phase transformation in responding to the sintering temperature and time is likely to be more prominent when using α-Al_2O_3 as the sintering precursor because of the resultant reduction in the diffusion barrier and the potential enhancement offered by the surface diffusion mechanism.

Leaching Behavior of CuO, Cu_2O, $CuAl_2O_4$, and $CuAlO_2$. A preferred method for evaluating the effect of copper immobilization after incorporation into different hosting phases is to compare the leachability of single-phase samples in prolonged leaching environments. Thus, this study prepared the Cu-containing phases that had occurred in previous

sintering sections, specifically CuO, Cu_2O, $CuAl_2O_4$, and $CuAlO_2$, to further evaluate their copper stabilization effects. To ensure the successful fabrication of single-phase samples, a longer sintering time was used to facilitate the complete copper transformation in the products. A 60 h sintering process was carried out to synthesize a Cu_2O sample from the CuO powder at 1020 °C. A mixture of CuO and γ-Al_2O_3 at a molar ratio of Cu:Al = 1:1 was heated at 1120 °C for 96 h to obtain the single-phase $CuAlO_2$ sample. A sintering temperature of 990 °C was used to fabricate the $CuAl_2O_4$ sample and prevent the formation of $CuAlO_2$. A relatively low sintering temperature led to a 20 d sintering process that successfully fabricated the single-phase $CuAl_2O_4$ sample shown in Figure S5 of the Supporting Information. To normalize the solid surface area factor during the leaching process, all samples were homogenized by grinding them into their powdered forms, with surface area measurements of 0.17 $m^2\ g^{-1}$ for CuO, 0.43 $m^2\ g^{-1}$ for Cu_2O, 1.35 $m^2\ g^{-1}$ for $CuAl_2O_4$, and 0.39 $m^2\ g^{-1}$ for $CuAlO_2$ samples. The pH value responses in the leaching fluid after the leaching processes are shown in Figure 6a. Within the first few days, the pH values for the CuO and Cu_2O leachates experienced significant increases from 2.9 to 4.7−4.9. In contrast, the pH values of the $CuAl_2O_4$ and $CuAlO_2$ leachates generally remained very close to the leaching fluid's initial pH throughout the entire leaching period. Because such an increase in leachate pH is usually accompanied by the destruction of a sample's crystal structure, the increase in the CuO and Cu_2O leachate pH may indicate lower capabilities of the CuO and Cu_2O phases to resist proton-mediated dissolution compared to the capabilities of the $CuAl_2O_4$ and $CuAlO_2$ phases.

As the same sample weight (0.5 g) was used in all leaching experiments, the copper fraction in each sample, subject to the different copper phases, can be normalized for comparison similarly to the sample surface area factor. Therefore, the copper leachability results from this study were expressed as leached copper over total copper in the sample per sample surface area (mg/g m^{-2}) as shown in Figure 6b. The leached copper from the CuO and Cu_2O phases was also observed to elevate quickly after 18 h of leaching. The amount of copper leached from the CuO phase was over 400 times higher than that from the $CuAl_2O_4$ phase and was about 100 times higher than that in the $CuAlO_2$ leachates at the end of the leaching period. Although the normalized copper concentrations in the Cu_2O leachates were lower than those in the CuO leachates, the Cu_2O phase generally still possessed a very high vulnerability toward acidic environments. The leaching results without normalization are provided in Figure 6c and show that the leached copper amounts from the oxide forms were still significantly higher than those from the aluminates. The results in Figure 6b and c confirm that both $CuAl_2O_4$ and $CuAlO_2$ phases had much higher intrinsic resistances to acidic attack when compared to the CuO and Cu_2O phases. Furthermore, with or without surface area normalization, the leached copper amounts from $CuAl_2O_4$ were even lower than those from $CuAlO_2$. Therefore, the $CuAl_2O_4$ structure proved to be the most stable form for immobilizing the hazardous copper among the four hosting phases that appeared in this aluminum-rich ceramic sintering process.

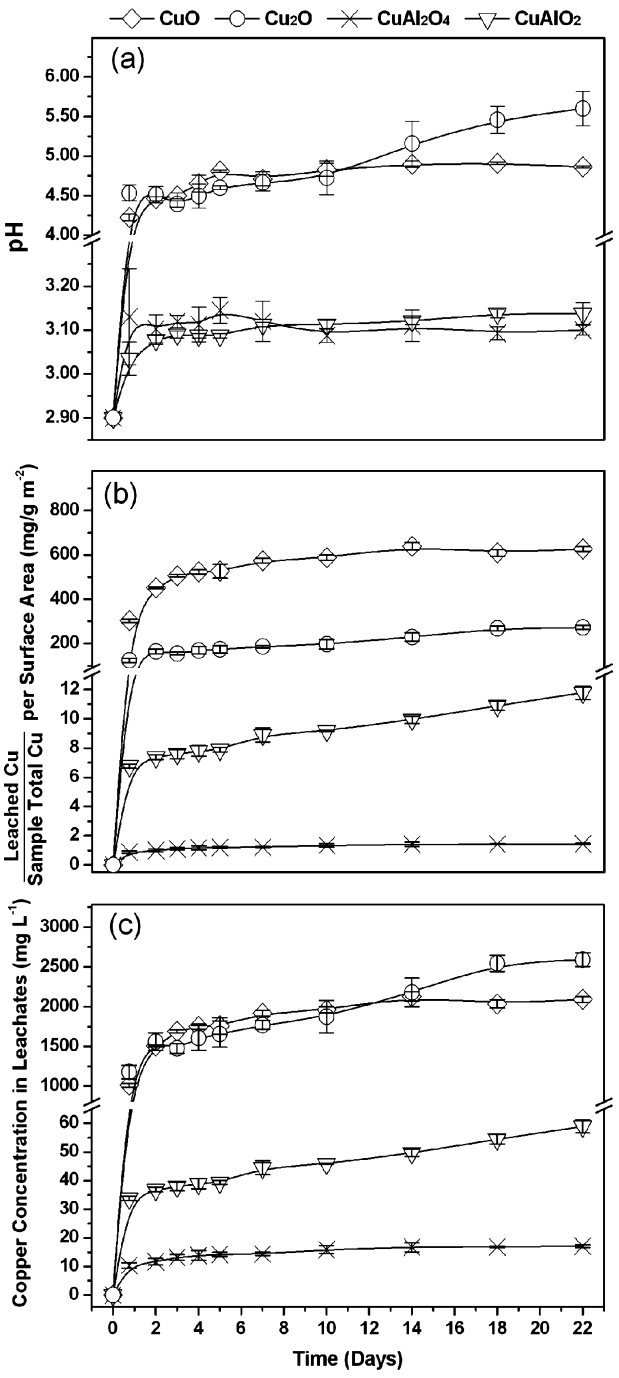

Figure 6. Variations of (a) leachate pH values, (b) leached Cu/sample total Cu per surface area, and (c) Cu concentrations in the leachates of CuO, Cu_2O, $CuAl_2O_4$, and $CuAlO_2$ samples. The leaching solution was TCLP extraction fluid #2 (acetic acid solution) at pH 2.9. Each leaching vial was filled with 10 mL of extraction fluid and 0.5 g of powder, then tumbled end-over-end from 0.75 to 22 d.

CONCLUSIONS

Hazardous copper was successfully incorporated into the $CuAl_2O_4$ spinel structure using alumina precursors during a 3 h sintering scheme. The maximum production of the $CuAl_2O_4$ phase was observed at 1000 and 1050 °C for the γ-Al_2O_3 and α-Al_2O_3 systems, respectively. Competitive formations of $CuAl_2O_4$ and $CuAlO_2$ occurred in the system, and the reaction sequences performed differently depending on whether γ-Al_2O_3 or α-Al_2O_3 was used as the sintering precursor. The development of the $CuAlO_2$ phase was predominantly caused by the decomposition of $CuAl_2O_4$ spinel in the γ-Al_2O_3 precursor system. Using the α-Al_2O_3 precursor under prolonged sintering prompted a decrease in the $CuAlO_2$

phase and a corresponding increase in $CuAl_2O_4$ spinel at the boundary temperature (1100 °C) of Cu(I) reoxidation. When comparing the sintering behavior of the CuO + γ-Al_2O_3 and CuO + α-Al_2O_3 systems, the temperature for $CuAl_2O_4$ formation was generally lower in the γ-Al_2O_3 system due to the lower energy input needed for the CuO and γ-Al_2O_3 interaction. The fully dense microstructure of the products sintered from the γ-Al_2O_3 system indicates a greater diffusion barrier to phase transformation compared to the very porous products that used α-Al_2O_3 as the precursor.

The pH values of the CuO and Cu_2O leachates quickly elevated to reach around pH 5 after the 22 d leaching period. In contrast, the pH values of the $CuAl_2O_4$ and $CuAlO_2$ leachates remained very close to pH 2.9 throughout the entire leaching period. With the additional assistance of normalized copper leaching data, the intrinsic copper leachability of the $CuAl_2O_4$ and $CuAlO_2$ phases were confirmed to be much lower than those of the CuO and Cu_2O phases. The performance of the copper aluminates in the prolonged leaching experiment shows that copper can be more securely immobilized in aluminate phases to resist the proton-mediated dissolution. With the goal of safely incorporating metal waste into the existing industrial processing for marketable ceramic products, this waste-to-resource study may create a more economically viable and environmentally sustainable strategy toward the management of metal-bearing waste. This result also suggests a possible strategy to incorporate copper-laden sludge into an aluminum-rich matrix using a short sintering scheme with attainable temperatures in the ceramic industry. With the key metal stabilization mechanisms and reaction sequences delineated in this work, future work using real sludge should be carried out to explore the effect of the sludge matrix discharged from different waste streams.

■ ASSOCIATED CONTENT

Supporting Information

One table and seven figures demonstrating the powder XRD patterns of the precursors used, selected sintered samples, and examples of the Rietveld refinement procedure. This material is available free of charge via the Internet at http://pubs.acs.org.

■ AUTHOR INFORMATION

Corresponding Author

*E-mail: kshih@hku.hk. Tel.: +852-2859-1973. Fax: +852-2559-5337.

Notes

The authors declare no competing financial interest.

■ ACKNOWLEDGMENTS

This work was financially supported by the General Research Fund Scheme (HKU 716310E) and the Special Equipment Grant (SEG_HKU10) from the Research Grants Council of Hong Kong. The Alcoa Corporation's contribution of HiQ-7223 alumina is gratefully acknowledged.

■ REFERENCES

(1) Park, D.; Lee, D. S.; Park, J. M.; Chun, H. D.; Park, S. K.; Jitsuhara, I.; Miki, O.; Kato, T. Metal recovery from electroplating wastewater using acidophilic iron oxidizing bacteria: Pilot-scale feasibility test. *Ind. Eng. Chem. Res.* **2005**, *44*, 1854−1859.

(2) Okuno, N.; Ishikawa, Y.; Shimizu, A.; Yoshida, M. Utilization of sludge in building material. *Water Sci. Technol.* **2004**, *49*, 225−232.

(3) Shih, K.; Leckie, J. O. Nickel aluminate spinel formation during sintering of simulated Ni-laden sludge and kaolinite. *J. Eur. Ceram. Soc.* **2007**, *27*, 91−99.

(4) Shih, K.; White, T.; Leckie, J. O. Spinel formation for stabilizing simulated nickel-laden sludge with aluminum-rich ceramic precursors. *Environ. Sci. Technol.* **2006**, *40*, 5077−5083.

(5) Shih, K.; White, T.; Leckie, J. O. Nickel stabilization efficiency of aluminate and ferrite spinels and their leaching behavior. *Environ. Sci. Technol.* **2006**, *40*, 5520−5526.

(6) Tang, Y.; Shih, K.; Chan, K. Copper aluminate spinel in the stabilization and detoxification of simulated copper-laden sludge. *Chemosphere* **2010**, *80*, 375−380.

(7) Tang, Y.; Chui, S. S.-Y.; Shih, K.; Zhang, L. Copper stabilization via spinel formation during the sintering of simulated copper-laden sludge with aluminum-rich ceramic precursors. *Environ. Sci. Technol.* **2011**, *45*, 3598−3604.

(8) Jacob, K. T.; Alcock, C. B. Thermodynamics of $CuAlO_2$ and $CuAl_2O_4$ and phase equilibria in the system Cu_2O−CuO−Al_2O_3. *J. Am. Ceram. Soc.* **1975**, *58*, 192−195.

(9) Völtzke, D.; Abicht, H.-P. Mechanistic investigations on the densification behaviour of barium titanate ceramics. *Solid State Sci.* **2001**, *3*, 417−422.

(10) Aksel, C.; Kasap, F.; Sesver, A. Investigation of parameters affecting grain growth of sintered magnesite refractories. *Ceram. Int.* **2005**, *31*, 121−127.

(11) Sun, D. D.; Tay, J. H.; Cheong, H. K.; Leung, D. L. K.; Qian, G. R. Recovery of heavy metals and stabilization of spent hydrotreating catalyst using a glass-ceramic matrix. *J. Hazard. Mater.* **2001**, *B87*, 213−223.

(12) Pavlov, V. F.; Alekseeva, L. L.; Mitrokhin, V. S. Influence of the firing conditions upon the heat resistance of ceramic articles. *Glass Ceram.* **1975**, *32* (10), 674−676.

(13) Sakata, M.; Cooper, M. J. An analysis of the Rietveld profiles refinement method. *J. Appl. Crystallogr.* **1979**, *12*, 554−556.

(14) Wiles, D. B.; Young, R. A. A new computer program for Rietveld analysis of X-ray powder diffraction patterns. *J. Appl. Crystallogr.* **1981**, *14*, 149−151.

(15) Neumann, R.; Costa, G. E.; Gaspar, J. C.; Palmieri, M.; Silva, S. E. The mineral phase quantification of vermiculite and interstratified clay minerals-containing ores by X-ray diffraction and Rietveld method after K cation exchange. *Miner. Eng.* **2011**, *24*, 1323−1334.

(16) Guirado, F.; Galí, S.; Chinchón, S. Quantitative Rietveld analysis of aluminous cement clinker phases. *Cem. Concr. Res.* **2000**, *30*, 1023−1029.

(17) Taylor, J. C.; Hinczak, I. *Rietveld Made Easy: A Practical Guide to Understanding the Method and Successful Phase Quantifications*; Sietronics Pty Ltd.: Belconnen ACT, Australia, 2003.

(18) MacKenzie, K. J. D.; Temuujin, J.; Smith, M. E.; Angerer, P.; Kameshima, Y. Effect of mechanochemical activation on the thermal reactions of boehmite (γ-AlOOH) and γ-Al_2O_3. *Thermochim. Acta* **2000**, *359*, 87−94.

(19) Tsuchida, T.; Furuichi, R.; Sukegawa, T.; Furudate, M.; Ishii, T. Thermoanalytical study on the reaction of the CuO-Al_2O_3(η, γ and α) systems. *Thermochim. Acta* **1984**, *78*, 71−80.

(20) Susnitzky, D. W.; Carter, C. B. The formation of copper aluminate by solid-state reaction. *J. Mater. Res.* **1991**, *6*, 1958−1963.

(21) Sarıkaya, Y.; Ada, K.; Önal, M. A model for initial-stage sintering thermodynamics of an alumina powder. *Powder Technol.* **2008**, *188*, 9−12.

(22) McHale, J. M.; Navrotsky, A. Effects of increased surface area and chemisorbed H_2O on the relative stability of nanocrystalline g-Al_2O_3 and α-Al_2O_3. *J. Phys. Chem. B* **1997**, *101*, 603−613.

(23) Zhou, R. S.; Snyder, R. L. Structures and transformation mechanisms of the η, γ and θ transition aluminas. *Acta Crystallogr.* **1991**, *B47*, 617−630.